Mitochondrial DNA depletion causes decreased ROS production and resistance to apoptosis

HULIN CHEN[1*], JUNLING WANG[2*], ZHONGRONG LIU[1], HUILAN YANG[1], YINGJIE ZHU[1], MINLING ZHAO[1], YAN LIU[1] and MIAOMIAO YAN[1]

[1]Department of Dermatology, Guangzhou General Hospital of Guangzhou Military Command (Liuhuaqiao Hospital), Guangzhou, Guangdong 510010; [2]Gynecologic Department of Guangzhou Hospital of Integrated Traditional and West Medicine, Guangzhou, Guangdong 510800, P.R. China

Received July 19, 2015; Accepted June 14, 2016

DOI: 10.3892/ijmm.2016.2697

Abstract. Mitochondrial DNA (mtDNA) depletion occurs frequently in many diseases including cancer. The present study was designed in order to examine the hypothesis that mtDNA-depleted cells are resistant to apoptosis and to explore the possible mechanisms responsible for this effect. Parental human osteosarcoma 143B cells and mtDNA-deficient (Rho° or ϱ°) 206 cells (derived from 143B cells) were exposed to different doses of solar-simulated ultraviolet (UV) radiation. The effects of solar irradiation on cell morphology were observed under both light and fluorescence microscopes. Furthermore, apoptosis, mitochondrial membrane potential (MMP) disruption and reactive oxygen species (ROS) production were detected and measured by flow cytometry. In both cell lines, apoptosis and ROS production were clearly increased, whereas MMP was slightly decreased. However, apoptosis and ROS production were reduced in the Rho°206 cells compared with the 143B cells. We also performed western blot analysis and demonstrated the increased release of cytosolic Cyt *c* from mitochondria in the 143B cells compared with that in the Rho°206 cells. Thus, we concluded that Rho°206 cells exhibit more resistance to solar-simulated UV radiation-induced apoptosis at certain doses than 143B cells and this is possibly due to decreased ROS production.

Introduction

Mitochondrial DNA (mtDNA) is comprised of a circular molecule of approximately 16.6 kb, encoding RNAs and polypeptides of the mitochondrial respiratory chain. Intact mtDNA is necessary for the production of these polypeptides, which consist of the key catalytic subunits of the mitochondrial respiratory chain complexes and are essential for oxidative ATP production. The mtDNA is frequently exposed to oxidative stress due to the process of oxidative phosphorylation. During oxidative phosphorylation, molecular oxygen is transformed into highly reactive oxygen species (ROS) in the electron transport chain, resulting in the damage of functional macromolecules including DNA (1).

The occurrence of mtDNA variation during evolution, particularly with regard to the normal variation in its amount, is closely associated with cell physiology and human health. Over the past 20 years, researchers have found that a number of disorders in humans are associated with severe mtDNA depletion and that long-term exposure to low concentrations of ethidium bromide (EB) establishes mtDNA-deficient (Rho° or ϱ°) cells (2). Thus, ϱ° cells have been used to examine the roles of mtDNA and particularly the importance of mtDNA in apoptosis (3). A previous study showed that respiration-deficient cells resisted tumor necrosis factor (TNF)/serum deprivation-induced apoptosis, whereas apoptosis was initiated in parental cells and rescued cells with normal mtDNA (4). These findings suggest that mtDNA depletion is involved in a mechanism responsible for resistance to apoptosis. Furthermore, studies by Amuthan *et al* and Biswas *et al* demonstrated that mtDNA depletion contributed to tumor progression and metastasis (5,6). Thus, it is likely that mtDNA depletion prevents apoptosis and generates cancer-related proteins.

Organisms may be exposed to numerous noxious agents under various conditions. These agents not only passively disintegrate cells, but also induce productive responses. In particular, it has been shown in mammalian cells that several genes are activated by ultraviolet (UV) irradiation (7).

Taking all of the above into consideration, this study was designed to examine the hypothesis that mtDNA-depleted mammalian cells resist UV-induced apoptosis and to explore the possible mechanism responsible for this effect.

Materials and methods

Cell culture, reagents and antibodies. The human parental osteosarcoma cell line 143B and Rho°206 cells

Correspondence to: Mr. Zhongrong Liu, Department of Dermatology, Guangzhou General Hospital of Guangzhou Military Command (Liuhuaqiao Hospital), 111 Liuhua Road, Guangzhou, Guangdong 510010, P.R. China
E-mail: pfklzr@163.com

*Contributed equally

Key words: DNA depletion, mitochondrial, ultraviolet, apoptosis, reactive oxygen species

Table I. UVA + UVB intensity, exposure time and dosage.

Experimental grouping	Intensity (UVA + UVB mW/cm^2)	Exposure time (min)	Dosage (mJ/cm^2+J/cm^2)
Sham-irradiation group (SIG)	0+0	0	0+0
Low-dose groups (LDG)			
IG1	2.95+56.5	1	177+3.39
IG2	2.95+56.5	2	354+6.78
High-dose groups (HDG)			
IG3	2.95+56.5	3	531+10.17
IG4	2.95+56.5	4	708+13.56

(mtDNA-depleted) were a gift from Professor Minxin Guan (Zhejiang University, Zhejiang, China). The cells were cultured in Dulbecco's modified Eagle's medium (Invitrogen, Carlsbad, CA, USA) supplemented with 10% newborn calf serum (Gibco, Carlsbad, CA, USA), 100 U/ml penicillin, 100 mg/ml streptomycin, 100 μg/ml bromodeoxyuridine and 50 μg/ml uridine (Sigma-Aldrich, St. Louis, MO, USA). Rhodamine 123 (Rh123) and dichlorodihydrofluorescein diacetate (DCFH-DA) were purchased from Sigma Chemical Co. (St. Louis, MO, USA). 3-(4,5-Dimethylthiazol-2-yl)-2,5-diphenyltetrazolium bromide (MTT) was purchased from Promega (Madison, WI, USA). We purchased cytochrome *c* (Cyt *c)* antibodies (12963S) from Cell Signaling Technology (CST; Beverly, MA, USA). Antibodies against β-actin (AA128) and the secondary horseradish peroxidase (HRP)-labeled antibodies (A0216), were purchased from Beyotime Biotechnology (Jiangsu, China).

Irradiation procedure. The irradiation procedure was performed using a 1000 Watt Solar Oriel UV Simulator (Oriel, Stratford, CT, USA) with a UVX digital radiometer (Ultra-Violet Products, Upland, CA, USA) which was equipped with a UVX-310 sensor to measure UV radiation intensity. The intensities of UVA and UVB were 2.95 and 56.6 mW/cm^2, respectively, with doses ranging from 177 mJ/cm^2 and 3.39 J/cm^2 to 708 mJ/cm^2 and 13.56 J/cm^2, respectively (Table I). The cells were washed twice with phosphate-buffered saline (PBS) prior to UV irradiation and then covered with a thin film of PBS during UV irradiation. Following irradiation, PBS was removed and immediately replaced with the maintenance medium. The sham-irradiated cells (control group) were similarly treated; however, they were exposed to normal room lighting. Finally, all the cells were incubated at 37˚C in an incubator with 5% CO_2 (Thermo Fisher Scientific, Waltham, MA, USA).

Cell viability assay. As previously described, the MTT method (8) was performed to measure cell viability. Prior to adding MTT tetrazolium salt to each well at a working concentration of 5 mg/ml, the cells were seeded in 96-well plates at a density of 5x10^5 cells/cm^2 overnight and treated with UV as indicated in Table I with a 4 h incubation time in a CO_2 incubator. Subsequently, the medium in each well was replaced with 150 μl DMSO (Sigma-Aldrich). The absorbance of the dissolved formazan crystals in each well was measured using a plate reader (Dynatech MR5000; Dynex Technologies, Chantilly, VA, USA) at a test wavelength of 570 nm. Cell viability was calculated using the following equation: (absorbance of the experiment samples/absorbance of the control) x100%.

Measurement of mitochondrial membrane potential (MMP). The cationic lipophilic green fluorochrome Rh123 is an effective reagent used to determine MMP (9). Prior to incubating with 10 μM Rh123 at 37˚C for 30 min, the cells were harvested and washed three times with PBS. Following incubation, the cells were washed twice with PBS and fluorescence was determined using a flow cytometer (Beckman Coulter, Inc., Brea, CA, USA) with an excitation wavelength of 488 nm through the FL-1 filter.

Determination of intracellular ROS levels. DCFH-DA is a reliable reagent which was used to determine intracellular ROS levels as previously described (10). The cells were incubated with DCFH-DA (10 μM) at 37˚C for 30 min. Following incubation, the cells were washed with PBS twice and the fluorescence of dichlorofluorescein (DCF) generated by ROS was analyzed immediately using a flow cytometer through the FL-1 filter with an excitation wavelength of 488 nm.

Annexin V-PE/7-AAD staining. Apoptosis was determined by flow cytometric analysis (BD Biosciences, Franklin Lakes, NJ, USA) with Annexin V-PE and 7-AAD double staining. After the cells were harvested and washed twice with ice-cold PBS, the cells were stained and fluorescence was measured at an excitation wavelength of 480 nm through the FL-1 filter (530 nm) and FL-2 filter (585 nm).

Assessment of cell morphology and PCR identification. Cell morphology was assessed using a fluorescence microscope and an electron microscope (Jeol, Peabody, MA, USA). For microscope observations, the cells were firstly observed under bright light after being cultured overnight in 24-well dishes and exposed to UV radiation as described in Table I, and subsequently observed under purple light after fixing and staining with DAPI (Beyotime Biotechnology) for 15 min.

For electron microscopy, the cells were fixed with 2% paraformaldehyde/2% glutaraldehyde in 0.1 M PBS,

followed by 1% OsO_4 (Sigma-Aldrich). Finally, the cells were stained with uranyl acetate (Sigma-Aldrich) and lead citrate (Sigma-Aldrich) for observation after dehydration, as previously described (11).

A volume of 20 μl containing 10 μl PrimeStar Max Premix 2X (Takara, Dalian, China) and 10 pmol of primer was added to amplify the COX II gene. The human mitochondrial COX II primers used in our study have been reported previously (12). The following sequences of COX II primers were used: forward, 5'-ATC AAA TCA ATT GGC CAC CAA TGG TA-3' and reverse, 5'-TTG ACC GTA GTA TAC CCC CGG TC-3' (297 bp). PCR was performed according to the manufacturer's instructions. The 200bp DNA Ladder (Dye Plus; Takara Bio, Otsu, Japan) was used to verify the bands.

Western blot analysis. The cells, at a density of $1x10^7$ cells/ml, were exposed to UV radiation as described in Table I. Following the lysis procedure, the lysates were centrifuged to obtain the supernatants. The protein concentrations of the supernatants were then determined using BCA Protein assay reagent (Beyotime Biotechnology). Western blot analysis was performed to analyze certain proteins in the supernatants (50 μg) of each sample.

Statistical analysis. Data are expressed as the means ± SD and analyzed using the Student's t-test (two-tailed). A P-value <0.05 was considered to indicate a statistically significant difference.

Results

Rho°206 cells exhibit greater resistance to apoptosis compared with 143B cells following exposure to UV radiation. Previous studies have shown that transient mtDNA depletion enhances the invasive ability of several types of cancer cells as well as resistance to apoptosis (5,13). Thus, it is evident that mtDNA-depleted cells play roles in tumor progression and metastasis. To the best of our knowledge, there are no studies regarding the effect of mtDNA depletion in human osteosarcoma 143B cells. To determine the anti-apoptotic effects of mtDNA depletion in 143B cells, we used Rho°206 cells, an mtDNA-depleted 143B cell type, as shown in Fig. 1.

Firstly, we observed the decrease in cell numbers in the two cell lines following exposure to UV radiation as described in Table I under a light microscope and a fluorescence microscope. Fig. 2A and B show that the numbers of 143B cells clearly decreased in comparison with the number of Rho°206 cells. Furthermore, MTT analysis showed the differences in the cell viability of Rho°206 and 143B cells following exposure to UV radiation. The cell viability of 143B cells was lower than that of Rho°206 cells (Fig. 2C). Additionally, Annexin V-PE and 7-AAD double staining by flow cytometry shows that the 143B cells endured more severe apoptosis compared with the Rho°206 cells following exposure to UV radiation (Fig. 2D and E). This may indicate that Rho°206 cells are more resistant to apoptosis.

UV-induced disruption of MMP is reduced in Rho°206 cells compared with that in 143B cells. To detect changes in MMP in the cells following UV irradiation in the present study, we measured MMP by assessing the uptake of Rh123 using a flow cytometer.

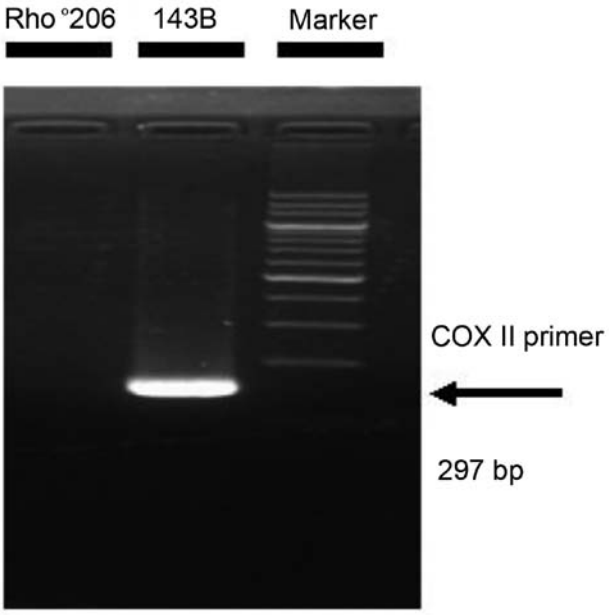

Figure 1. Verification of mitochondrial DNA (mtDNA)-depletion in Rho°206 cells. The mtDNA-encoded gene COX II was amplified by PCR. A 297 bp band containing the COX II sequence was detected in the DNA isolated from 143B cells whereas it was lost in the DNA isolated from Rho°206 cells.

Following exposure to UV radiation as described in Table I, mitochondrial activity was decreased in both cell lines. As shown in Fig. 3, following exposure to different intensities of radiation, the 143B cells displayed various disruptions of MMP. Compared with the control, mitochondrial activity decreased to 76.35% after 708 mJ/cm^2 UVA and 13.56 J/cm^2 UVB treatment (IG4 group) in the 143B cells, and to 85.1% in the Rho°206 cells. The impact of the combination of 708 mJ/cm^2 UVA and 13.56J/cm^2 UVB on mitochondrial activity in the 143B cells (Fig. 3B and C) suggested that UV caused the decline in mitochondrial activity. At the same time, no significant disruption of MMP was detected after 708 mJ/cm^2 UVA and 13.56 J/cm^2 UVB treatment in both cell lines (data not shown), indicating that UV may exert a minimal effect on the MMP and mitochondrial dysfunction.

Furthermore, Fig. 3 shows clearly that the MMP in the 143B cells dropped more quickly than in the Rho°206 cells following UV irradiation from which we concluded that mtDNA depletion may protect cells against UV-induced disruption of MMP.

UV irradiation induces less ROS production in Rho°206 cells compared with that in 143B cells. Disruptions in MMP and cell apoptosis are associated with the production of ROS (14,15). Thus, in the present study, we measured ROS production in the 143B cells and the Rho°206 cells following exposure to UV radiation as described in Table I. The oxidation sensitive fluorescent dye DCFH-DA was applied in order to evaluate ROS production. ROS production was significantly increased in both cell lines following exposure to increasing doses of UV radiation. In the 143B cells, the generation of ROS was faster compared with that in the

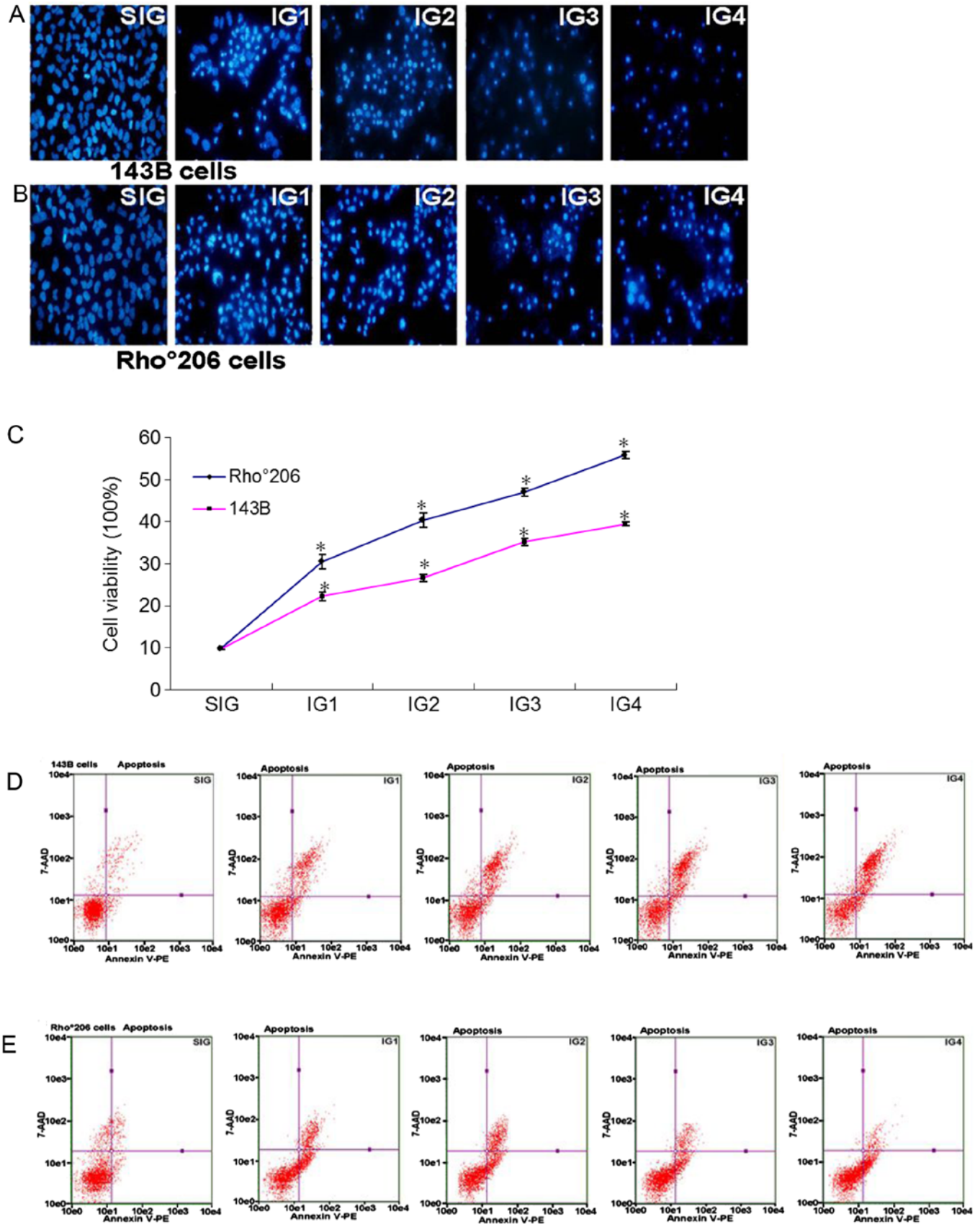

Figure 2. Ultraviolet (UV) irradiation induces various degrees of cell death in 143B and Rho°206 cells. (A) Effect of solar-simulated UV irradiation on the morphology of 143B cells observed under a fluorescence microscope (x40 magnification). (B) Morphological changes showed in Rho°206 cells following treatment with solar-simulated UV irradiation under a fluorescence microscope (x40). (C) MTT analysis of 143B and Rho°206 cells following solar-simulated UV irradiation. *P<0.05 vs. SIG control. Each bar represents the means ± SD from three experiments. Annexin V-PE and 7-AAD staining for apoptosis in (D) 143B and (E) Rho°206 cells following simulated solar irradiation. x-axis, Annexin V-PE; y-axis, DNA content by 7-AAD. The experiment was repeated three times and the image presented is typical of these three independent tests.

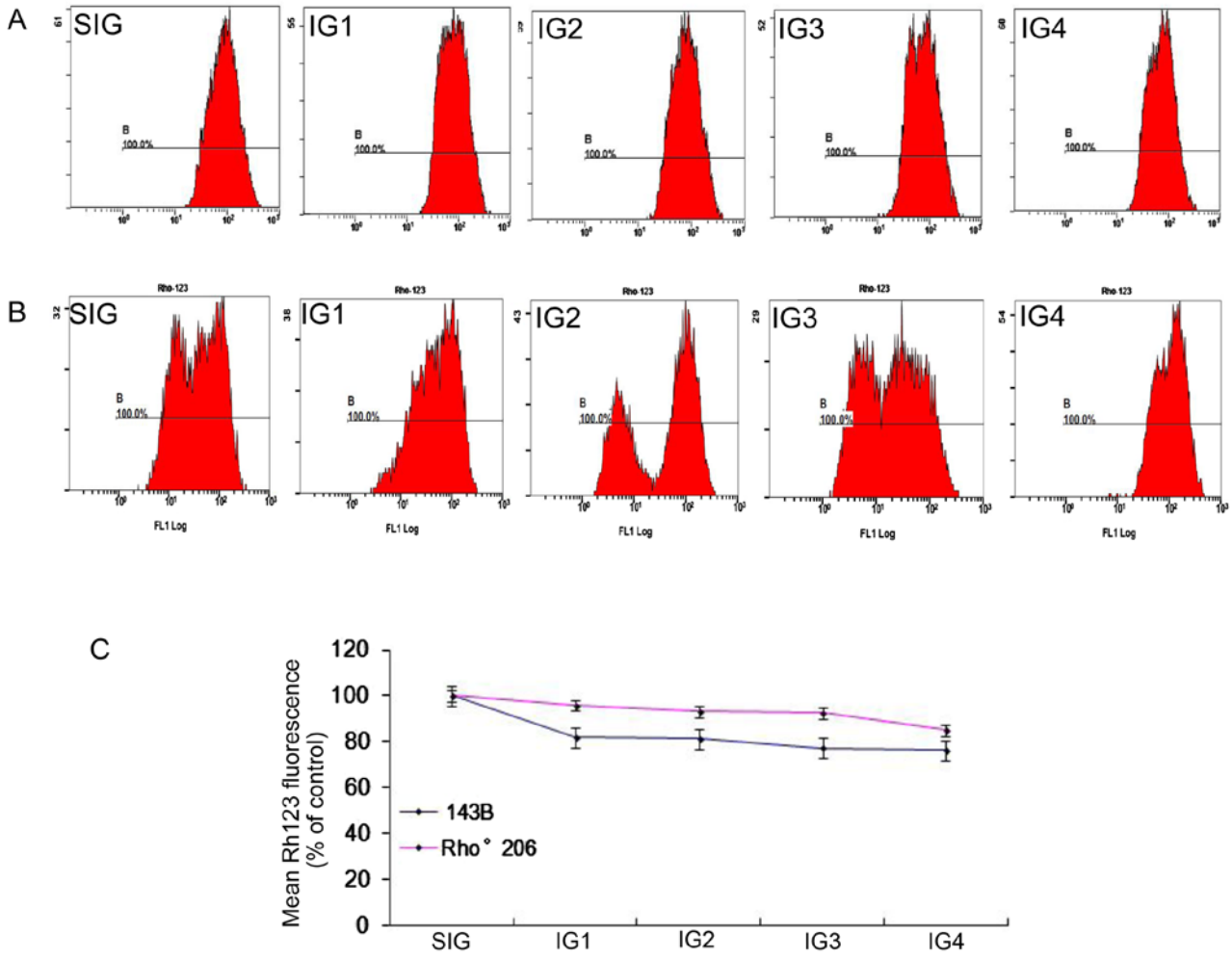

Figure 3. Effects of combined treatment with ultraviolet radiation (UVA and UVB) on the mitochondrial membrane potential (MMP). (A) Rho°206 and (B) 143B cells were seeded at a concentration of 1x10^6 cells/ml, and then exposed different doses of UV irradiation (Table I). After three washes, the cells were incubated at 37˚C for 30 min with 10 μM rhodamine 123 (Rh123) in PBS. The fluorescence was measured using flow cytometry (excitation wavelengths were both 488 nm, and emission wavelengths were both 525 nm). The test was repeated three times and the image presented is representative of these three independent tests. Each bar represents the means ± SD from three experiments. (A and B) There were signficant changes in MMP in both cell lines at different doses of UV radiation. (C) A comparison between 143B and Rho°206 cell lines shows that there was no significant difference in MMP between the SIG groups (P>0.05). However, there were significant differences between the cell lines at the same irradiation doses.

control group after UV exposure, (an approximate 3-5-fold increase), as shown in Fig. 4A and C. In the Rho°206 cells, there was an approximate 2-4-fold increase in the generation of ROS compared with the control group (Fig. 4B and C). These results show that ROS production increased more rapidly in 143B cells compared with that in Rho°206 cells following UV irradiation.

Rho°206 cells resist UV-induced apoptosis through decreasing Cyt c release. During apoptosis, Cyt *c* is released from mitochondria into the cytoplasm (16). To examine whether Cyt *c* was released during UVA combined with UVB-induced cell apoptosis, the expression of cytosolic Cyt *c* was measured using western blot analysis. Increased levels of Cyt *c* in the cytoplasm were detected following exposure to a combination of UVA and UVB (Fig. 5) compared with the controls. This increase was more evident in the parental 143B cells than in the mtDNA-depleted Rho°206 cells, indicating a potential resistance to Cyt *c* release in the Rho°206 cells. Furthermore, the morphological changes observed in the mitochondria of the Rho°206 cells (Fig. 6) may not be conducive to Cyt *c* release in these cells.

Discussion

Previous findings have demonstrated that mtDNA encodes pivotal catalytic subunits and its complete depletion in cells leads to several morphological changes. Fig. 6 shows that the mitochondrial density of mtDNA-depleted Rho°206 cells was reduced and that the mitochondria were larger and more elongated compared with those in the parental 143B cells. Hojo *et al* also observed similar changes in cyclosporin-treated cells (17). Furthermore, a major block also occurs in the normal electron flow in mtDNA-depleted cells.

Mitochondria are the principal source of intracellular ROS under adverse conditions (18,19). This, in combination with the fact that excision repair frequently occurs in mtDNA (20), suggests that mtDNA is liable to attack under conditions of oxidative and chemical stress. A number of studies regarding homoplasmic/heteroplasmic mtDNA depletion/mutations have

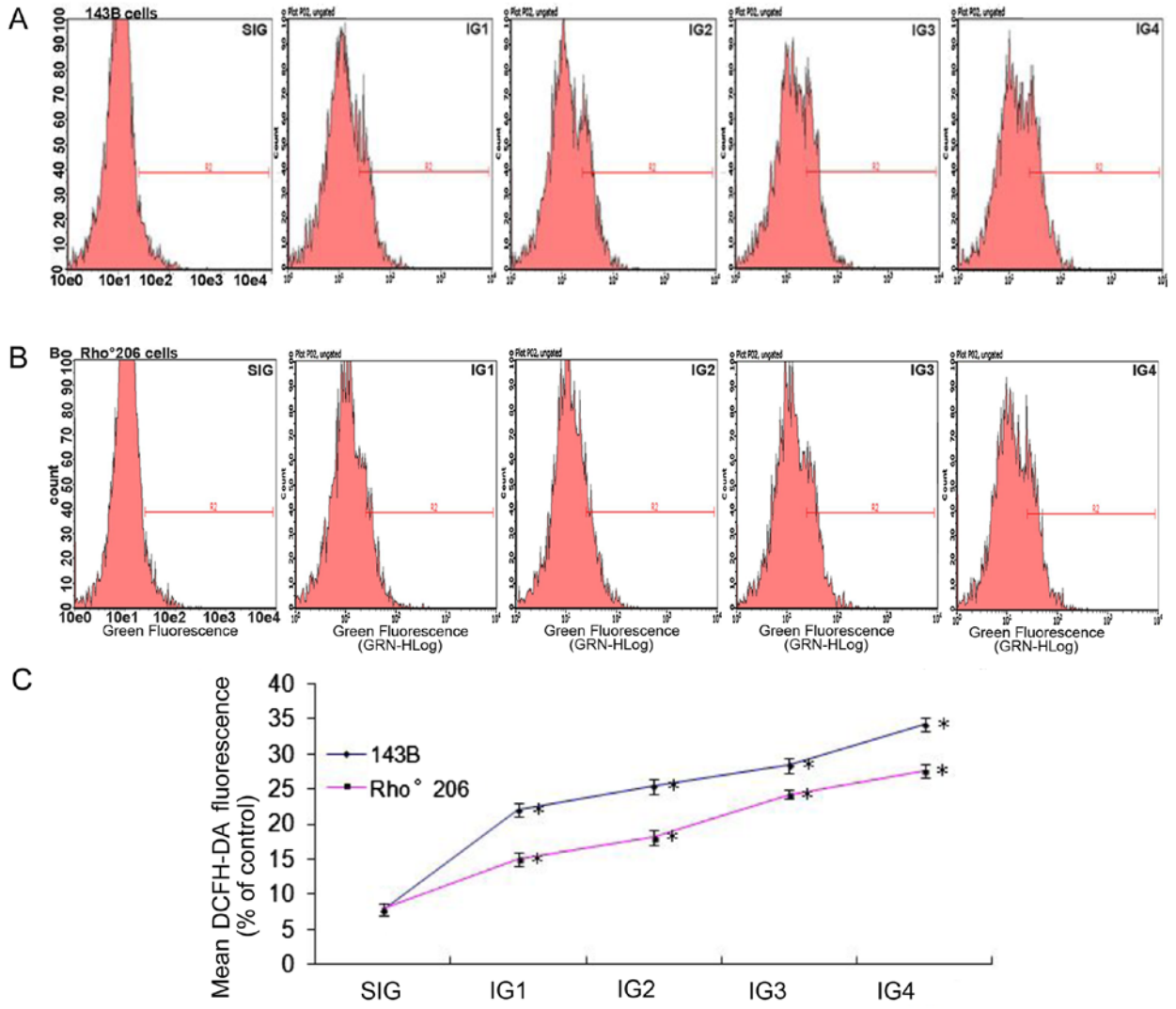

Figure 4. Exposure to ultraviolet (UV) radiation increases the production of reactive oxygen species (ROS). (A) 143B and (B) Rho°206 cells were seeded at a density of $1x10^6$ cells/ml, and then exposed to different doses of UV (Table I). After three washes, the cells were incubated at 37˚C for 30 min with 10 μM DCFH-DA in PBS. The fluorescence was measured using flow cytometry (excitation wavelengths were both 488 nm, and emission wavelengths were both 525 nm). (C) A comparison between 143B and Rho°206 cell lines shows that there was no significant difference in ROS production between the SIG groups (P>0.05). However, there were significant differences between the cell lines at the same irradiation doses. *P<0.05 vs. SIG control. The test was repeated three times and the image presented is representative of these three independent tests. Each bar represents the means ± SD from three experiments.

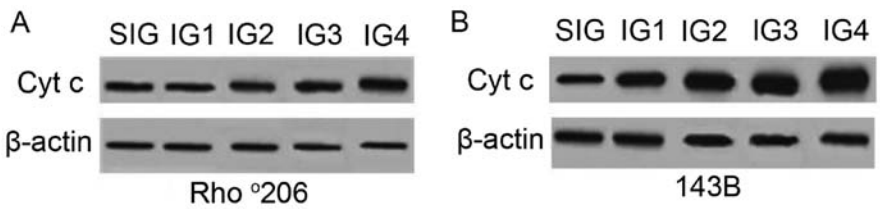

Figure 5. Effects of ultraviolet (UV) irradiation on the levels of cytochrome c (Cyt *c)* in the two cell lines. (A) Rho°206 cells and (B) 143B were exposed to different doses of UV radiation (Table I). The cytosolic fractions of Cyt *c*. were measured using western blot analysis. The experiment was repeated three times and the image presented is representative of these three independent tests.

been reported in human tumors which support this view (21-27). However, it remains unclear whether cancer progression results in (28) or from (29) the depletion/mutations. The results presented in this study suggest that mtDNA-depleted cells possess a survival advantage following environmental exposure to UV irradiation.

UV irradiation is a pivotal factor that increases levels of ROS (30-35), and simultaneously decreases antioxidant enzymes (36), causing oxidative stress to initiate cellular signal transduction. Redundant ROS are likely to lead to cell death by oxidizing and then damaging functional macromolecules such as DNA and protein. Herein, we found that UV

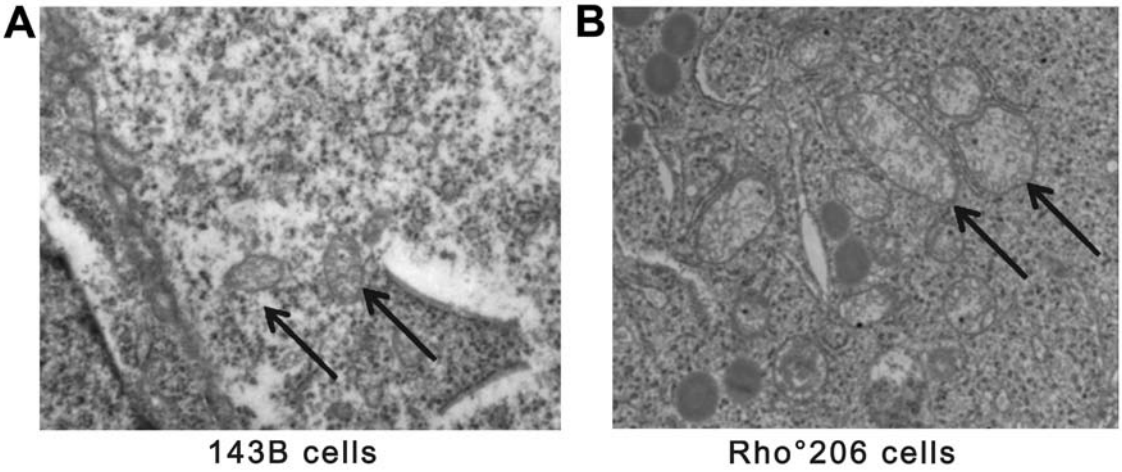

Figure 6. A transmission electron microscopic comparison of 143B and Rho°206 cells. (A) x20,000 magnification of 143B cells showing elongated mitochondria with parallel ordered cristae and normal electron density (indicated by black arrows). (B) x20,000 magnification of Rho°206 cells. Mitochondria have an irregular cristae pattern and a 'whorled appearance' and are enlarged with almost complete or partial loss of the internal cristae structural pattern. Cytoplasmic vacuoles are enlarged and appear more numerous in (B) compared with (A).

exposure induced ROS production in human mammalian cells and mtDNA-depleted cells resisted the release of ROS thereby escaping greater death compared with the normal cells. Notably, UV irradiation in 143B cells and Rho°206 cells had minor effects on MMP, since MMP disruption is always followed by increasing ROS levels (37). This paradox warrants further investigation. We also observed Cyt *c* release, as previously described (37). Notably, the 143B cells released more Cyt *c* from the mitochondria into the cytoplasm than the Rho°206 cells following UV irradiation. Therefore, it is possible that DNA depletion in mitochondria induces resistance to UV-induced apoptosis by decreasing ROS production, which plays a role in the upstream apoptotic mechanism following Cyt *c* release and the activation of caspases.

Acknowledgements

The present study was supported by the National Science Foundation of China (NSFC, grant no. 30972652), and the Science and Technology Department of Guangdong Province Program (no. 2013B021800053).

References

1. Orrenius S, Gogvadze V and Zhivotovsky B: Mitochondrial oxidative stress: implications for cell death. Annu Rev Pharmacol Toxicol 47: 143-183, 2007.
2. King MP and Attardi G: Human cells lacking mtDNA: repopulation with exogenous mitochondria by complementation. Science 246: 500-503, 1989.
3. Chandel NS and Schumacker PT: Cells depleted of mitochondrial DNA (ϱ°) yield insight into physiological mechanisms. FEBS Lett 454: 173-176, 1999.
4. Higuchi M, Aggarwal BB and Yeh ET: Activation of CPP32-like protease in tumor necrosis factor-induced apoptosis is dependent on mitochondrial function. J Clin Invest 99: 1751-1758, 1997.
5. Amuthan G, Biswas G, Zhang SY, Klein-Szanto A, Vijayasarathy C and Avadhani NG: Mitochondria-to-nucleus stress signaling induces phenotypic changes, tumor progression and cell invasion. EMBO J 20: 1910-1920, 2001.
6. Biswas G, Anandatheerthavarada HK, Zaidi M and Avadhani NG: Mitochondria to nucleus stress signaling: a distinctive mechanism of NFkappaB/Rel activation through calcineurin-mediated inactivation of IkappaBbeta. J Cell Biol 161: 507-519, 2003.
7. Friedberg E, Walker G and Siede W: DNA repair and mutagenesis. ASM Press, Washington, DC, 1995.
8. Shi Y, Wang CH and Gong XG: Apoptosis-inducing effects of two anthraquinones from *Hedyotis diffusa* WILLD. Biol Pharm Bull 31: 1075-1078, 2008.
9. Lu M, Gong X, Lu Y, Guo J, Wang C and Pan Y: Molecular cloning and functional characterization of a cell-permeable superoxide dismutase targeted to lung adenocarcinoma cells. Inhibition cell proliferation through the Akt/p27kip1 pathway. J Biol Chem 281: 13620-13627, 2006.
10. Li J, Xu Z, Tan M, Su W and Gong XG: 3-(4-(Benzo[d) thiazol-2-yl)-1-phenyl-1H-pyrazol-3-yl) phenyl acetate induced Hep G2 cell apoptosis through a ROS-mediated pathway. Chem Biol Interact 183: 341-348, 2010.
11. Gong K, Chen C, Zhan Y, Chen Y, Huang Z and Li W: Autophagy-related gene 7 (ATG7) and reactive oxygen species/extracellular signal-regulated kinase regulate tetrandrine-induced autophagy in human hepatocellular carcinoma. J Biol Chem 287: 35576-35588, 2012.
12. Lewis LD, Hamzeh FM and Lietman PS: Ultrastructural changes associated with reduced mitochondrial DNA and impaired mitochondrial function in the presence of 2'3'-dideoxycytidine. Antimicrob Agents Chemother 36: 2061-2065, 1992.
13. Amuthan G, Biswas G, Ananadatheerthavarada HK, Vijayasarathy C, Shephard HM and Avadhani NG: Mitochondrial stress-induced calcium signaling, phenotypic changes and invasive behavior in human lung carcinoma A549 cells. Oncogene 21: 7839-7849, 2002.
14. Xiong Y, Liu X, Lee CP, Chua BH and Ho YS: Attenuation of doxorubicin-induced contractile and mitochondrial dysfunction in mouse heart by cellular glutathione peroxidase. Free Radic Biol Med 41: 46-55, 2006.
15. López E, Arce C, Oset-Gasque MJ, Cañadas S and González MP: Cadmium induces reactive oxygen species generation and lipid peroxidation in cortical neurons in culture. Free Radic Biol Med 40: 940-951, 2006.
16. Li P, Nijhawan D, Budihardjo I, Srinivasula SM, Ahmad M, Alnemri ES and Wang X: Cytochrome *c* and dATP-dependent formation of Apaf-1/caspase-9 complex initiates an apoptotic protease cascade. Cell 91: 479-489, 1997.
17. Hojo M, Morimoto T, Maluccio M, Asano T, Morimoto K, Lagman M, Shimbo T and Suthanthiran M: Cyclosporine induces cancer progression by a cell-autonomous mechanism. Nature 397: 530-534, 1999.
18. Kehrer JP: Free radicals as mediators of tissue injury and disease. Crit Rev Toxicol 23: 21-48, 1993.
19. Lenaz G: Role of mitochondria in oxidative stress and ageing. Biochim Biophys Acta 1366: 53-67, 1998.
20. Pinz KG and Bogenhagen DF: Efficient repair of abasic sites in DNA by mitochondrial enzymes. Mol Cell Biol 18: 1257-1265, 1998.

21. Allen JA and Coombs MM: Covalent binding of polycyclic aromatic compounds to mitochondrial and nuclear DNA. Nature 287: 244-245, 1980.
22. Backer JM and Weinstein IB: Mitochondrial DNA is a major cellular target for a dihydrodiol-epoxide derivative of benzo[a] pyrene. Science 209: 297-299, 1980.
23. Niranjan BG, Bhat NK and Avadhani NG: Preferential attack of mitochondrial DNA by aflatoxin B1 during hepatocarcinogenesis. Science 215: 73-75, 1982.
24. Horton TM, Petros JA, Heddi A, Shoffner J, Kaufman AE, Graham SD Jr, Gramlich T and Wallace DC: Novel mitochondrial DNA deletion found in a renal cell carcinoma. Genes Chromosomes Cancer 15: 95-101, 1996.
25. Polyak K, Li Y, Zhu H, Lengauer C, Willson JK, Markowitz SD, Trush MA, Kinzler KW and Vogelstein B: Somatic mutations of the mitochondrial genome in human colorectal tumours. Nat Genet 20: 291-293, 1998.
26. Fliss MS, Usadel H, Caballero OL, Wu L, Buta MR, Eleff SM, Jen J and Sidransky D: Facile detection of mitochondrial DNA mutations in tumors and bodily fluids. Science 287: 2017-2019, 2000.
27. Yeh JJ, Lunetta KL, van Orsouw NJ, Moore FD Jr, Mutter GL, Vijg J, Dahia PL and Eng C: Somatic mitochondrial DNA (mtDNA) mutations in papillary thyroid carcinomas and differential mtDNA sequence variants in cases with thyroid tumours. Oncogene 19: 2060-2066, 2000.
28. Loeb LA: A mutator phenotype in cancer. Cancer Res 61: 3230-3239, 2001.
29. Rasmussen AK, Chatterjee A, Rasmussen LJ and Singh KK: Mitochondria-mediated nuclear mutator phenotype in *Saccharomyces cerevisiae*. Nucleic Acids Res 31: 3909-3917, 2003.
30. Masaki H, Atsumi T and Sakurai H: Detection of hydrogen peroxide and hydroxyl radicals in murine skin fibroblasts under UVB irradiation. Biochem Biophys Res Commun 206: 474-479, 1995.
31. Jurkiewicz BA and Buettner GR: EPR detection of free radicals in UV-irradiated skin: mouse versus human. Photochem Photobiol 64: 918-922, 1996.
32. Barber LA, Spandau DF, Rathman SC, Murphy RC, Johnson CA, Kelley SW, Hurwitz SA and Travers JB: Expression of the platelet-activating factor receptor results in enhanced ultraviolet B radiation-induced apoptosis in a human epidermal cell line. J Biol Chem 273: 18891-18897, 1998.
33. Brenneisen P, Wenk J, Klotz LO, Wlaschek M, Briviba K, Krieg T and Scharffetter-Kochanek K: Central role of ferrous/ferric iron in the ultraviolet B irradiation-mediated signaling pathway leading to increased interstitial collagenase (matrix-degrading metalloprotease (MMP)-1) and stromelysin-1 (MMP-3) mRNA levels in cultured human dermal fibroblasts. Biol Chem 273: 5279-5287, 1998.
34. Yasui H and Sakurai H: Chemiluminescent detection and imaging of reactive oxygen species in live mouse skin exposed to UVA. Biochem Biophys Res Commun 269: 131-136, 2000.
35. Kang S, Chung JH, Lee JH, Fisher GJ, Wan YS, Duell EA and Voorhees JJ: Topical N-acetyl cysteine and genistein prevent ultraviolet-light-induced signaling that leads to photoaging in human skin in vivo. J Invest Dermatol 120: 835-841, 2003.
36. Yamamoto Y: Role of active oxygen species and antioxidants in photoaging. J Dermatol Sci 27: 1-4, 2001.
37. Chandra D, Liu JW and Tang DG: Early mitochondrial activation and cytochrome c up-regulation during apoptosis. J Biol Chem 277: 50842-50854, 2002.